

Comparison of individual pitch and smart rotor control strategies for load reduction

C Plumley¹, W Leithead¹, P Jamieson¹, E Bossanyi² and M Graham³

¹Strathclyde University, Royal College Building, 204 George Street, Glasgow, G1 1XW, UK

²St Vincent's Works, Silverthorne Lane, BS2 0QD, Bristol, UK

³Imperial College London, South Kensington Campus, London, SW7 2AZ, UK

E-mail: charles.plumley@strath.ac.uk

Abstract. Load reduction is increasingly seen as an essential part of controller and wind turbine design. On large multi-MW wind turbines that experience high levels of wind shear and turbulence across the rotor, individual pitch control and smart rotor control are being considered. While individual pitch control involves adjusting the pitch of each blade individually to reduce the cyclic loadings on the rotor, smart rotor control involves activating control devices distributed along the blades to alter the local aerodynamics of the blades. Here we investigate the effectiveness of using a DQ-axis control and a distributed (independent) control for both individual pitch and trailing edge flap smart rotor control. While load reductions are similar amongst the four strategies across a wide range of variables, including blade root bending moments, yaw bearing and shaft, the pitch actuator requirements vary. The smart rotor pitch actuator has reduced travel, rates, accelerations and power requirements than that of the individual pitch controlled wind turbines. This benefit alone however would be hard to justify the added design complexities of using a smart rotor, which can be seen as an alternative to upgrading the pitch actuator and bearing. In addition, it is found that the independent control strategy is apt at roles that the collective pitch usually targets, such as tower motion and speed control, and it is perhaps here, in supplementing other systems, that the future of the smart rotor lies.

1. Introduction

Wind turbines have been progressively getting larger in a drive to reduce the cost of energy. Rotor diameters of 120m plus are now in operation and at these sizes the wind field experienced by each blade as it rotates varies considerably. This is due to wind shear, turbulence, tower-shadow, yaw, wake from other wind turbines or obstructions up stream, and from other meteorological effects. These cause periodic loadings on the turbine as the blades experience a similar, though varying, wind field once per revolution.

The cyclic loadings cause damage to the blades in particular, but also to the tower, yaw bearing and shaft. To mitigate these loads advanced control strategies are being considered. Individual pitch control and smart rotor control are two such methods, adoption of which may allow blades to be made cheaper and lighter, or longer still, reducing the overall cost of energy from wind turbines, e.g. [1].



1.1. Individual pitch control

Individual pitch control is a method whereby each blade has its own pitch angle. This is possible when each blade has an independent pitch actuator, which for modern multi-MW turbines is common. As such, implementing an individual pitch control does not require an expensive redesign.

Collective pitch control is used for speed regulation, which is set by a central controller, while individual pitch control supplements this collective pitch control signal and is designed to reduce loadings on the wind turbine. A number of different methods for individual pitch control have been proposed, with positive results [2], [3], [4]. Individual pitch control has been implemented on real wind turbines, though there is still some concern over the robustness of the controller, and a fear that excessive use of the pitch actuator could result in excessive pitch bearing wear [5]. The additional demands put on the actuator that could lead to such problems are considered in Section 4.2 of this paper in comparison to the base case and to the case when the smart rotor control is active.

1.2. Smart rotor control

The smart rotor consists of control devices distributed along the blades of the wind turbine, allowing real-time adjustment of the aerodynamic characteristics of the blades. There are a couple of obvious drawbacks though. Firstly there is the risk of faults, downtime and what could be costly maintenance, although a recent study has shown this is not necessarily the case [6]. Secondly the smart rotor could require expensive redesign of the blades, but again it is possible a robust device may be developed that is both cheap and easy to implement. A review of various devices can be found in [7] and [8]. At the moment the most likely candidate for early adoption is the trailing edge flap, much like the aileron on an aircraft wing, which has a long history and has been implemented on the two demonstration plants in operation: a Vestas V-27 in Denmark (225kW) [9], and a Zond-750 (750kW) at Sandia Laboratories in New Mexico [10].

Trailing edge flaps have been shown to demonstrate load reduction potential by a number of authors with results comparable to those of individual pitch control e.g. [11], [12]. The question then arises though, as to whether this complex smart rotor system is of merit when the results are only comparable to individual pitch control. One method to avoid this question is to simply make the smart rotor an extension of individual pitch control, i.e. supplementing it to achieve greater load reductions. This has been tried with promising results [13], [14], but equal load reduction gains can be had simply by making the pitch actuators work harder. A method to compare the costs associated with upgrading the pitch system or implementing a smart rotor is therefore needed.

In this paper individual pitch and smart rotor control strategies are comprehensively compared side-by-side to highlight the alterations required to a baseline wind turbine to achieve set out-of-plane blade root bending moment load reductions using either control strategy. This is done through a comparison of actuator requirements, power variability and of loads on the turbine.

2. Baseline wind turbine

For the comparisons a baseline controller and wind turbine are needed. The UpWind/NREL 5MW wind turbine is actively used by academia, freely available and large enough to make advanced controller techniques important. It is based on the NREL 5MW described in [15] with minor additions where required. The key characteristics are shown in Table 1. The wind turbine and controller are modelled in Bladed [16], an industry standard wind turbine package.

To model the smart rotor a single flap is added to each blade. These are located on the outboard section of the 61.5 m blades between 47.3 m and 57.3 m with a chord width of 10%, capable of $\pm 30^\circ$ deflections at a maximum rate of $\pm 60^\circ/s$. The aerodynamic characteristics of

Table 1: Characteristics of NREL 5MW reference wind turbine

| | |
|-----------------------------------|------------------------------------|
| Rating | 5 MW |
| Rotor orientation, configuration | Upwind, 3 blades |
| Control | Variable speed, collective pitch |
| Drivetrain | High speed, multiple-stage gearbox |
| Rotor, hub diameter | 126m, 3m |
| Hub height | 90m |
| Cut-in, rated, cut-out wind speed | 3 m/s, 11.4 m/s, 25 m/s |
| Cut-in, rated rotor speed | 6.9 rpm, 12.1 rpm |
| Rated tip speed | 80 m/s |
| Overhang, shaft tilt, precone | 5 m, 5 degrees, 2.5 degrees |
| Rotor mass | 110,000 kg |
| Nacelle mass | 240,000 kg |
| Tower mass | 347,460 kg |
| Coordinate location of overall CM | (-0.2 m, 0.0 m, 64.0 m) |

these flaps are determined using XFOIL [17], before input into Bladed as look-up tables with data between points being interpolated.

These values are chosen due to the trailing edge flap's similarity with ailerons, elevators and rudders on large commercial jets, which are of a similar scale [18]. However, the characteristics of smart rotor devices varies significantly [7], [8], and indeed the flap characteristics can also be quite different dependent on their design [19], [20]. Nonetheless, should similar control strategies to those presented in this work be used with different smart rotor devices, the effect on the pitch actuator and loads should still be similar.

3. Control Strategies

The baseline controller used is based on the UpWind 5MW design, described in the report by Bossanyi [21], with the exception that in the above rated region torque is held constant to avoid the risk of destabilising the system. Two advanced controller designs are considered: a DQ-axis centralised controller and a distributed controller, whereby the actuators are controlled independently of each other and so termed an independent controller here. Both of these strategies are taken from individual pitch control, whereby the blades are pitched individually rather than collectively, but they can equally be applied to smart rotor control, wherein the active control surface is a flap or other device, whilst the pitch is still controlled collectively.

These controllers are phased out below rated from 100% at rated power, to 0% action at 80% rated power. This is so as not to disrupt optimum energy capture, but also because there is less to be gained in this operating region as the loads below rated power are low. This may be adjusted dependent on a economic assessment of the trade-off between energy capture and load reduction.

3.1. DQ-axis control

The DQ-axis control strategy used for the flaps is adopted from studies involving individual pitch control e.g. [2]. The rotating blade root bending moment of each blade is converted to tilt and yaw moments in a stationary plane using the Coleman transform. The magnitude of these vectors then depict the asymmetrical yaw and tilt load components. Proportional Integral (PI) controllers then act to minimise these tilt and yaw moments, before the inverse Coleman transform is used to set the demand angle for each blade. The DQ-axis control and independent control are set-up identically for both the pitch and smart rotor controls, with the exception

that the demand for the actuators is switched from pitch to flap control and the gains increased by a factor of 8 for the smart rotor case. A visual representation of this strategy is shown in Figure 1.

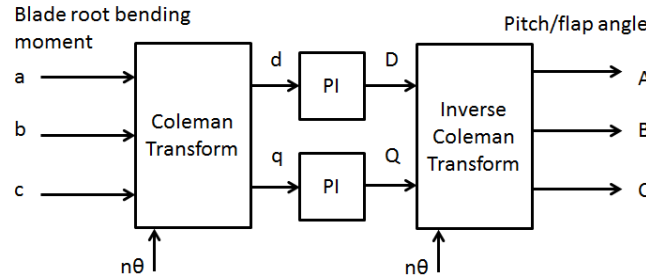


Figure 1: Schematic of the DQ-axis control method

The Coleman transformation, otherwise known as the Park’s or DQ-0 transform, is

$$\begin{bmatrix} d \\ q \end{bmatrix} = \frac{2}{3} \begin{bmatrix} \cos(\theta) & \cos(\theta + \frac{2\pi}{3}) & \cos(\theta + \frac{4\pi}{3}) \\ \sin(\theta) & \sin(\theta + \frac{2\pi}{3}) & \sin(\theta + \frac{4\pi}{3}) \end{bmatrix} \begin{bmatrix} a \\ b \\ c \end{bmatrix} \quad (1)$$

where θ is the rotor azimuth angle, a , b , and c are the blade root bending moments of the each of the three blades, and d and q are the transformed fixed axis loadings, in the yaw and tilt directions respectively. The inverse transform is

$$\begin{bmatrix} A \\ B \\ C \end{bmatrix} = \begin{bmatrix} \cos(\theta) & \sin(\theta) \\ \cos(\theta + \frac{2\pi}{3}) & \sin(\theta + \frac{2\pi}{3}) \\ \cos(\theta + \frac{4\pi}{3}) & \sin(\theta + \frac{4\pi}{3}) \end{bmatrix} \begin{bmatrix} D \\ Q \end{bmatrix} \quad (2)$$

where A , B and C are the demanded pitch/flap angles for each of the blades. An offset may be added to the inverse transform to account for controller delays, ωT , however this was found to have negligible impact on the load reduction potential of the controller. This controller effectively eliminates 1P loadings. Higher harmonic loadings may be reduced by altering the transform such that θ is multiplied by a factor, i.e. n to remove nP loads. To simplify analysis, reduce actuator requirements and due to the fact 1P loads cause the most significant amount of damage, only the 1P loads are targeted in this work.

3.2. Independent control

An alternative control approach is an independent control system. The collective pitch is still defined by the central controller, but then the actuator of each blade, or flap in the smart rotor design, attempts to maintain a set blade root bending moment for this pitch demand. The control system is displayed in Figure 2.

The conversion between pitch angle and bending moment is taken into account by a blade model. In this case the blade model is produced by fitting a curve to the relationship between collective pitch angle, β (in radians), and the blade root bending moment, My_{ref} (in MNm), during steady state operation. It is defined in the above rated region by the equation

$$My_{ref} = 32\beta^2 - 33\beta + 11 \quad (3)$$

The controller can then be adjusted to target specific frequencies, for example 1P vibrations. This can further be extended to decouple the smart rotor control from the wind turbine dynamics with what are termed fictitious forces, which take account of variations in the bending moment due to rotor and tower accelerations [3].

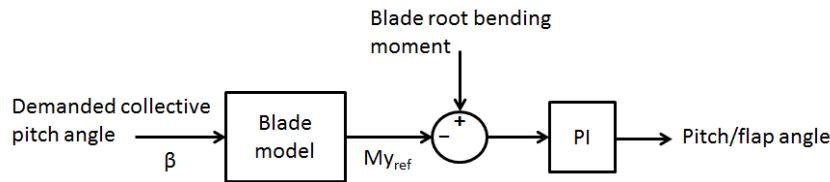


Figure 2: Distributed control scheme

4. Results

In simulations the design load case 1.2 from the IEC 61400 certification standard is used [22], as this case looks at fatigue damage for which the smart rotor and individual pitch control are primarily designed. The 1Hz damage equivalent loads are calculated and compared in the results. 3D turbulent Kaimal spectrum wind fields for a class IIB turbine are used, but rather than lifetime loads the results presented here are of just 6 runs at 18m/s mean wind speed. This mean wind speed was chosen as a first step prior to complete analysis and is representative of operation in the above rated region in which the advanced control strategies operate to their full potential.

There are a number of different metrics that could be used to highlight the effectiveness of the control strategies: load reductions, actuator requirements and power variability are selected here; and these are discussed in the following subsections.

4.1. Load reductions

The control objective of these advanced techniques is to reduce blade root out-of-plane loads. However, the goal of this work is to compare the different control strategies. By making the blade root out-of-plane load reductions deliberately similar for both the individual pitch and smart rotor, a direct comparison can be made between the two in other areas. This avoids bias that can occur simply by selecting favourable gains for one control type over another. Some interesting results can then be seen, even within the remit of loads, as displayed in Table 2.

Table 2: Damage equivalent loads compared to collective pitch control as a percentage (%)

| Load metric | DQ-axis control | | Independent control | |
|-----------------|-----------------|-------------|---------------------|-------------|
| | Pitch | Smart rotor | Pitch | Smart rotor |
| Blade root Mx | 96.2 | 96.3 | 103.3 | 102.0 |
| Blade root My | 79.5 | 79.7 | 84.6 | 88.6 |
| Rotating hub My | 73.4 | 74.5 | 77.9 | 79.0 |
| Rotating hub Mz | 73.5 | 74.1 | 78.3 | 79.2 |
| Yaw bearing My | 92.9 | 94.7 | 88.1 | 89.9 |
| Yaw bearing Mz | 94.2 | 94.8 | 89.0 | 92.1 |
| Tower base Mx | 99.6 | 101.4 | 93.1 | 97.3 |
| Tower base My | 106.3 | 102.8 | 69.6 | 73.5 |

The DQ-axis control method reduces not only the targeted out-of-plane blade root bending moment (blade root My), but also slightly reduces in-plane blade root bending moment (blade root Mx), loads on the shaft (rotating hub My and Mz), and marginally reduces loads on the yaw bearing too, while the fore-aft tower moment (tower base My) undergoes a small increase

in loads. Similar results are seen when using the independent control method, with a few exceptions, blade root in-plane loads actually increase slightly, while the blade and shaft load reductions are lower, the yaw bearing and tower loads though are significantly reduced. This is due to the independent control supplementing the collective pitch control duty and emphasises the impact that advanced controller techniques can have on the wind turbine system. It also highlights the potential to use smart rotor control to target more than just blade load reduction, such as tower loads.

4.2. Actuator requirements

Although it is possible to reduce loads through higher bandwidth devices, both pitch and flap actuators are set with the same actuator model: a second order passive transfer function with a frequency of 1Hz and damping factor of 0.7. This allows the actuator motion, torque and power required to be directly compared.

Initially a comparison is made of the pitch motion as shown in Table 3 (top). The increased travel, pitch rate and accelerations required of the individual pitch control strategies over the baseline case will likely result in increased wear of the actuator and pitch bearing. Based on this criteria, the pitch system would need to be upgraded to operate an individual pitch control strategy. In contrast, it can be seen that when using a smart rotor control strategy, the motion required of the pitch actuator can be held close to the baseline case (DQ-axis control), or even reduced (independent control), which could help to reduce wear. The cost to upgrade the pitch system versus the cost of implementing a smart rotor system is key to the decision of one system over another, but equally it is vital to compare the cost of implementing either system to the savings made from reduced loads.

Table 3: Comparison of pitch actuator motion (top) and flap acutator motion (bottom) as a percentage (%) of the baseline collective pitch controlled wind turbine pitch actuator

| Metric | Baseline | Pitch | | Smart rotor | |
|------------------------|---------------------|---------|-------------|-------------|-------------|
| | | DQ-axis | Independent | DQ-axis | Independent |
| Pitch travel | $0.64^\circ s^{-1}$ | 247.0 | 258.4 | 102.3 | 87.3 |
| Pitch rate std | $0.81^\circ s^{-1}$ | 235.8 | 256.7 | 102.4 | 86.2 |
| Pitch rate max | $3.06^\circ s^{-1}$ | 196.3 | 222.2 | 104.4 | 83.9 |
| Pitch acceleration std | $2.00^\circ s^{-2}$ | 215.9 | 505.2 | 104.5 | 126.8 |
| Pitch acceleration max | $9.63^\circ s^{-2}$ | 175.5 | 377.5 | 102.6 | 112.0 |

| Metric | Absolute | | % of baseline pitch | |
|---|----------|-------------|---------------------|-------------|
| | DQ-axis | Independent | DQ-axis | Independent |
| Flap deflection max ($^\circ$) | 23.1 | 23.7 | - | - |
| Flap travel ($^\circ s^{-1}$) | 10.9 | 15.3 | 1717.6 | 2399.4 |
| Flap rate std ($^\circ s^{-1}$) | 13.0 | 18.8 | 1606.3 | 2317.7 |
| Flap rate max ($^\circ s^{-1}$) | 33.9 | 44.4 | 1107.6 | 1453.7 |
| Flap acceleration std ($^\circ s^{-2}$) | 31.6 | 86.8 | 1579.1 | 4333.0 |
| Flap acceleration max ($^\circ s^{-2}$) | 150.9 | 289.8 | 1567.5 | 3010.4 |

For the smart rotor, we also need to consider the flap actuator. In the smart rotor case the angular rate of motion is higher, this is because a 5 degree change in flap angle is not equivalent

to a 5 degree change in pitch angle. Indeed, this is why the gains are adjusted from the pitch to flap control, with a factor of 8 found to take account of the reduced span of the flap and the reduced gradient of lift coefficient versus pitch, which is shown in Figure 3. As can be seen in Table 3 (bottom), the motions are correspondingly increased; it is tricky to draw a direct comparison between the two though, as the flap does not provide speed control, but again a factor of 8 looks reasonable between the pitch and flap motions.

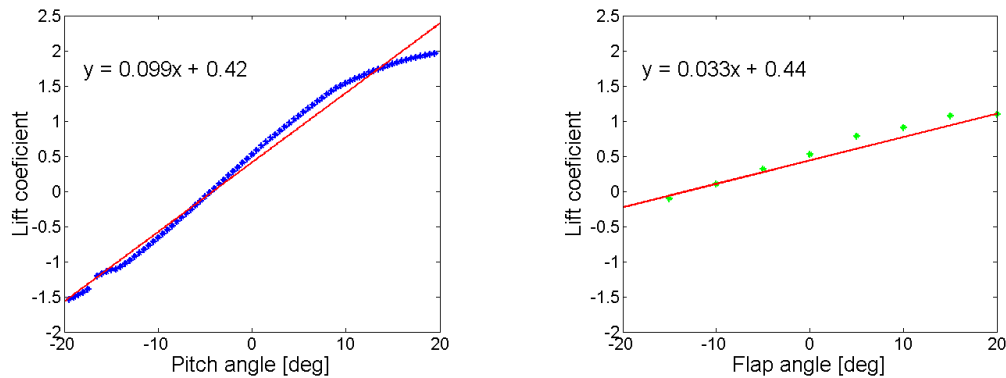


Figure 3: Lift coefficient versus pitch angle (L) and flap angle (R). The gradient of the pitch angle is steeper by a factor of 3

The torque requirements are somewhat different between the controllers too. The torques required depend on a number of factors: gravity loads, inertia, aerodynamic loads and friction. For the pitch actuator, these outputs are supplied by Bladed. For the flap actuator, the torques required for each of these is calculated as follows:

- Gravity loads: the centre of mass is calculated for the flap, the offset in the out-of-plane direction from the pivot point is then taken, and this is multiplied by the weight of the flap to calculate the torque, $\tau_{gravity}$. The out-of-plane displacement from the pivot point is calculated by taking into account the azimuth of the rotor, θ_{azi} , the pitch of the blade, θ_{blade} and the angle of the flap, θ_{flap} , such that $r = \cos(\theta_{azi})\sin(\theta_{blade} + \theta_{flap})$, and $\tau_{gravity} = r \times m_{flap}$, where m_{flap} is the mass of the flap.
- Inertial loads: the inertia of the flap is calculated and then this is multiplied by the angular acceleration of the flap, $\tau_{inertia} = I_{flap}\ddot{\theta}_{flap}$
- Aerodynamic loads: the hinge moment per unit span of the flap at different flap angles and angles of attack is given in XFOIL. This data is tabulated in a look-up table so that the aerodynamic torque on the flap may be calculated for various angles of attack and flap angles. The angle of attack of the blade is taken from Bladed outputs. The aerodynamic torque is also dependent on the chord length of the blade, c_{blade} , and the velocity of the perceived wind, v , which is also taken from Bladed for a series of blade sections. The equation used to calculate the aerodynamic moment on the flap hinge is then, $\tau_{aero} = \frac{1}{2}C_m(\alpha, \theta_{flap})\rho v^2 c_{blade}^2$, where ρ is the density of air.
- Friction: friction opposes the motion of the flap and is dependent on the type of bearing and actuator used. For example it might consist of a component of constant friction, friction coefficient proportional to the forces being applied and friction coefficient proportional to the rate of motion. As the type of bearing and actuator have not been considered in this paper, the frictional component is not considered here. It may however be a dominating component and would increase both torque and power consumption.

Table 4 shows the various components and the maximum torques required of the actuators for the various control cases for both the pitch and flap actuator.

Table 4: Component contributions to maximum torque demand of the actuators (Nm)

| Actuator | Inertia | Aerodynamic | Gravity | Total |
|------------|---------|-------------|---------|-------|
| CPC pitch | 380 | 9600 | 35 | 9600 |
| IPC pitch | 900 | 12000 | 38 | 12000 |
| IPCD pitch | 1300 | 7600 | 36 | 7700 |
| SRC pitch | 450 | 11000 | 35 | 11000 |
| SRCD pitch | 390 | 7700 | 35 | 7700 |
| SRC flap | 2 | 11 | 4 | 16 |
| SRCD flap | 3 | 11 | 7 | 18 |

CPC = baseline collective pitch control; IPC = DQ-axis individual pitch control; IPCD = independent pitch control; SRC = DQ-axis smart rotor control; SRCD = independent smart rotor control

The torque required of the actuators is dominated by the aerodynamic term when friction is ignored, which is a similar result to [10], with gravity loads being insignificant. Due to the small size of the flaps, the torques required are significantly lower than for that of the pitch control actuator. An interesting result though is that the torques required of the individual pitch control are not necessarily higher than the torques required of the collective pitch control. Suggesting the pitch actuators would not need to be updated as regards to their torque and indicating no benefit to using the smart rotor system over individual pitch control.

Nevertheless, the fact that the rotational speeds are different, mean that the power demands are also different. The maximum power demands for the different control systems are shown in Table 5.

Table 5: Power requirement of the pitch (first 5 columns) and flap actuator (last 2 columns)

| | CPC | IPC | IPCD | SRC | SRCD | SRC | SRCD |
|---------------|------|-------|------|------|------|-----|------|
| Max power (W) | 3600 | 10200 | 9400 | 4300 | 3000 | 7.6 | 11 |

Due to the increased motion of the individual pitch control the power consumption is higher than for the collective or smart rotor control cases. This increase will require better thermal dissipation and an actuator with a higher rated power.

Bearing and pitch actuator wear is a complex issue though. Whilst additional motion may increase wear, lower torques can reduce it, suggesting that a thorough analysis needs to be conducted into the exact causes and constraints on both the actuator and the bearings. As depending on the conditions and control strategy, wear might either increase or decrease and this will depend highly on the type of actuator and bearings under consideration. This will have a direct impact on the cost of adopting an individual pitch control strategy.

As regards to the flap actuator, the very low torque and power requirements are highly desirable, as if the actuator is to be integrated into the blade the space available will be constrained and lower torque and power requirements will allow a smaller actuator to be used. However, the high rates required of the actuators could be problematic. There is though the ability to trade increased torque for decreased movement through use of flaps with larger chord

and span lengths, so an optimum may be found here with a possible trade off between torque and motion. Equally leverage or gearing may be used.

4.3. Power variability

The final criteria for comparison here is power variability. Above rated pitch control is used to maintain rated rotor speed, whilst torque is held constant. Variations in speed therefore result in a change in power. It is found that power variability is similar regardless of the control strategy. A slight increase in variability with the DQ-axis controller is likely due to the pitch being required to target two separate criteria, speed control and loads, however, the independent control method facilitates reduction in power variability, as shown in Table 6. Again then this highlights the interesting opportunity to use the smart rotor control to supplement the tasks of the main pitch control, in this case speed control, and this is an area of future research.

Table 6: Wind turbine power outputs

| Control strategy | Mean power (kW) | Power std (kW) |
|------------------|-----------------|----------------|
| CPC | 5002.2 | 78.4 |
| IPC | 5002.3 | 80.6 |
| IPCD | 5001.7 | 69.1 |
| SRC | 5002.2 | 78.9 |
| SRCD | 5001.6 | 70.2 |

5. Conclusion

This study verifies that it is possible to achieve similar load reductions with trailing edge flaps as it is by pitching the entire blade. This was shown using two different control techniques: a DQ-axis centralised controller and a distributed controller. For individual pitch control, these come at a cost of increased actuator duty and power requirements, although torque demands are not necessarily increased. Any requirement to upgrade the pitch actuator and bearings will come at a cost, and it is these potential costs that need to be compared with the price attached to implementing a smart rotor in deciding which to adopt, if either.

From the results it is clear that use of trailing edge flaps can achieve the same load reductions without any alteration to the pitch actuator. Indeed use of the smart rotor can reduce both the motion and rates of the pitch actuator, creating potential savings. The flap actuator power and torque requirements are lower than for the pitch actuator by a few orders of magnitude, however the rates are much higher to achieve a similar load reduction. The real concern here is whether a suitable actuation system can be found that is both reliable and cost effective in comparison to upgrading the pitch system.

It is also shown that while load reductions are similar for the smart rotor and individual pitch, the style of the controller does have an effect on a variety of other variables, including components that are not the direct target of the controller. For instance tower loading and power variability. This encourages future work to look at the possibility of using the independent control technique to target a variety of loads, and in particular it could be interesting to explore the smart rotor's potential to supplement collective pitch control for roles other than out-of-plane blade root bending moment load reduction.

References

- [1] D. E. Berg, D. G. Wilson, F. Barone, Matthew, B. R. Resor, J. C. Berg, S. Kota, G. Ervin, and D. Maric, "The impact of active aerodynamic load control on fatigue and energy capture at low wind speed sites," tech. rep., US Government: Sandia National Laboratories, FlexSys Inc., USA.
- [2] E. Bossanyi, "Further load reductions with individual pitch control," *Wind Energy*, vol. 8, pp. 481–485, Oct. 2005.
- [3] W. E. Leithead, V. Neilson, S. Dominguez, and A. Dutka, "A novel approach to structural load control using intelligent actuators," in *17th Mediterranean Conference on Control & Automation*, no. June, (Thessaloniki, Greece), pp. 1257–1262, 2009.
- [4] T. J. Larsen, H. A. Madsen, and K. Thomsen, "Active load reduction using individual pitch, based on local blade flow measurements," *Wind Energy*, vol. 8, pp. 67–80, Jan. 2005.
- [5] M. Shan, J. Jacobsen, and S. Adelt, "Field Testing and Practical Aspects of Load Reducing Pitch Control Systems for a 5 MW Offshore Wind Turbine," 2013.
- [6] C. Plumley, W. Leithead, P. Jamieson, M. Graham, and E. Bossanyi, "Fault Ride-Through for a Smart Rotor DQ-axis Controlled Wind Turbine with a Jammed Trailing Edge Flap," in *EWEA*, 2014.
- [7] T. K. Barlas and G. a. M. van Kuik, "Review of state of the art in smart rotor control research for wind turbines," *Progress in Aerospace Sciences*, vol. 46, pp. 1–27, Jan. 2010.
- [8] S. J. Johnson, J. P. Baker, C. P. V. Dam, and D. E. Berg, "An overview of active load control techniques for wind turbines with an emphasis on microtabs," *Wind Energy*, vol. 13, no. August 2009, pp. 239–253, 2010.
- [9] D. Castaignet, T. Barlas, T. Buhl, N. K. Poulsen, J. J. Wedel-Heinen, N. A. Olesen, C. Bak, and T. Kim, "Full-scale test of trailing edge flaps on a Vestas V27 wind turbine: active load reduction and system identification," *Wind Energy*, pp. 2–6, 2013.
- [10] J. Berg, B. Resor, J. Paquette, and J. White, "SMART Wind Turbine Rotor: Design and Field Test," Tech. Rep. January, Sandia National Laboratories, Albuquerque, New Mexico and Livermore, California, 2014.
- [11] P. B. Andersen, L. Henriksen, and M. Gaunaa, "Deformable trailing edge flaps for modern megawatt wind turbine controllers using strain gauge sensors," *Wind Energy*, vol. 13, no. December 2009, pp. 193–206, 2010.
- [12] T. K. Barlas, G. J. van der Veen, and G. A. M. van Kuik, "Model predictive control for wind turbines with distributed active flaps: incorporating inflow signals," *Wind Energy*, vol. on-line, 2011.
- [13] M. A. Lackner and G. A. M. van Kuik, "A comparison of smart rotor control approaches using trailing edge flaps and individual pitch control," *Wind Energy*, vol. 13, no. July 2009, pp. 117–134, 2010.
- [14] D. G. Wilson, D. E. Berg, B. R. Resor, F. Barone, Matthew, and J. C. Berg, "Combined individual pitch control and active aerodynamic load controller investigation for the 5mw upwind turbine," in *AWEA Wind Power Conference*, (Chicago, Illinois), pp. 1–12, 2009.
- [15] J. Jonkman, S. Butterfield, W. Musial, and G. Scott, "Definition of a 5-MW Reference Wind Turbine for Offshore System Development," Tech. Rep. February, NREL, Colorado, 2009.
- [16] E. Bossanyi, "Bladed Theory Manual," tech. rep., DNV GL, Bristol, 2013.
- [17] M. Dreha, "XFOIL: An analysis and design system for low Reynolds number airfoils," in *Low Reynolds number aerodynamics*, (Notre Dame, IN, Germany), 1989.
- [18] D. Scholz, "Berechnung maximal erforderlicher Stellgeschwindigkeiten von Steuerflächen," in *Deutscher Luft und Raumfahrtkongreß*, (Munich), DGLR Jahrbuch, 1997.
- [19] S. Daynes and P. M. Weaver, "A morphing trailing edge device for a wind turbine," *Journal of Intelligent Material Systems and Structures*, vol. 23, pp. 691–701, Mar. 2012.
- [20] J. Berg, M. Barone, and N. Yoder, "SMART Wind Turbine Rotor: Data Analysis and Conclusions," Tech. Rep. January, Sandia National Laboratories, Albuquerque, New Mexico and Livermore, California, 2014.
- [21] E. Bossanyi, D. Witcher, and T. Mercer, "Project UpWind: Controller for 5MW reference turbine," Tech. Rep. July, Garrad Hassan and Partners Limited, Bristol, 2009.
- [22] IEC, "IEC 61400-1 Ed.3: Wind turbines - Part 1: Design requirements," 2005.